International Research Journal of Engineering and Technology (IRJET) e-ISSN: 2395-0056
Volume: 11 Issue: 03 | Mar 2024 www.irjet.net p-ISSN: 2395-0072

Seismic Performance Evaluation of RC MRF Under Near and Far-Field Ground Motions

Aftab Ahmad[1], Prof. Asif Husain[2]

[1]P.G. Student, Department of Civil Engineering, Jamia Millia Islamia, New Delhi, India
[2]Professor, Dept. of Civil Engineering, IIT Delhi, New Delhi, India

---

Abstract - *In seismic design and engineering, the choice of earthquake scenarios and soil conditions plays a pivotal role in ensuring the structural resilience of buildings. This study aims to develop seismic fragility curves and comprehensively evaluate the seismic response of an 8-storey structure situated on stiff soil, considering both far-fault and near-fault earthquake scenarios. The comparative analysis will shed light on the nuanced effects of ground motions originating at varying distances from the structure, offering valuable insights for seismic design and risk mitigation. For this purpose, Incremental dynamic analysis was performed and seismic fragility analysis of G+7 story moment resisting frame situated on stiff soil is utilized. Initially gravity, equivalent static and response spectrum analysis were conducted in order to design the building according to the national building code requirements then nonlinear static pushover analysis was carried out to see the failure modes and check if there are any local failures in the structure. structure's nonlinearity was modeled using lumped plasticity to simulate the inelastic behavior of beams and columns. Selection of near-field NP (Non-Pulse) and far-field ground motions was done according to ATC 63 using PEER nga-west database. IDA was performed for each group of ground motions and seismic fragility curves were developed. Modeling outcomes suggest that, in the case of two earthquakes sharing almost identical conditions, the near-fault record exhibits a greater array of displacement values. Near-fault ground motions exhibited higher recorded drift than far-field ground motions for same level of intensity both the overall and relative displacements show an incremental trend, and the significance of nonlinear behavior becomes more prominent, and the nonlinear range is achieved at lower percentile values.*

Key Words: Near-Fault; Seismic Fragility Curves; Incremental Dynamic Analysis (IDA); Dynamic Time History Analysis; Far-Fault

1.INTRODUCTION

In seismic studies, both near-field and far-field earthquakes hold pivotal importance, offering distinct challenges and considerations for structural engineering. Near-field earthquakes, occurring near the site of interest, exhibit higher ground accelerations and strong pulse-like motions with prominent directivity effects (Erdik, M., B. Şadan 2023) [1]. These seismic events, typically within a few tens of kilometers from the epicenter, pose unique challenges to structures, inducing nonlinear behavior and potential damage. On the other hand, far-field earthquakes, situated at a considerable distance, present different characteristics with lower ground accelerations, longer-duration shaking, and a broader frequency content (Bhairav, Thakur 2022) [2]. Their seismic waves experience less attenuation, resulting in a more gradual decay of ground motion amplitudes. Understanding the dynamics of both near-field and far-field earthquakes is essential for designing resilient structures. Engineers must tailor seismic design and retrofitting strategies to account for the concentrated and intense shaking of near-field events and the distributed, longer-duration shaking associated with far-field seismic waves, ensuring comprehensive resilience in seismically active regions. Seismic fragility analysis is needed to assess the probability of damage to structures during earthquakes and to estimate losses before and after an earthquake. Fragility models play a crucial role in performance-based earthquake engineering (PBEE) (V., Bui, Tran., Son 2022) [3] by representing the probability that the engineering demand parameter (EDP) exceeds a safety threshold given selected intensity measures (IMs). Various methods, such as empirical or analytical approaches, can be used to derive fragility curves that display the likelihood of different damage states being surpassed (Renato, Giannini., Fabrizio 2022) [4]. Dynamic analysis is commonly used to estimate fragility functions, and statistical inference methods can be applied to predict these functions and minimize the number of structural analyses needed. In order to calculate fragility functions, the definition of the limits states that characterize the state/performance of the structure is required. These limit states are defined in terms of an engineering demand parameter (i.e., a form of measure of the structure's response). In this study, the maximum Interstory drift was used. The corresponding EDP (drift) values are 1%, 2%, and 4% to define a state of Immediate occupancy, life safety, and collapse prevention respectively. These thresholds were obtained from FEMA 356 (Shakeba and Hamed 2022) [5]. Seismic fragility models can be used for risk and vulnerability assessment, disaster management, emergency preparedness, and retrofitting prioritization (Vamvatsikos and Cornell 2002) [6]. The objective of this research is to gather novel insights into the responses of reinforced concrete moment frames to near-fault ground motions and assess the variations compared to far-fault

ground motions. Specifically, the study emphasizes critical parameters such as maximum top displacements, inter-storey, drift ratios (IDR), probability of collapse, and responses obtained through incremental dynamic analysis (IDA) methodology.

1.1 Incremental Dynamic Analysis

Nonlinear response history analysis (NRHA) proves valuable in the seismic assessment of structures within the Incremental Dynamic Analysis (IDA) framework (Vamvatsikos and Cornell 2004) [7]. In IDA, the iterative application of NRHA involves employing a set of ground motions scaled to various factors, resulting in diverse responses at various levels of intensity are considered. Specifically, for any parameter used to describe the structural response in engineering (known as an Engineering Demand Parameter or EDP) and a measure of intensity (referred to as an IM), such as the 5% damped, first-mode spectral acceleration Sa (T1, 5%) (g), curves known as Incremental Dynamic Analysis (IDA) curves are created. These curves display the relationship between the EDP and IM for each record (as shown in Figure 1). Traditionally, the EDP, which is the variable dependent on the response, is plotted on the x-axis, while the IM, the independent variable representing intensity, is plotted on the y-axis. By examining these IDA curves, statistical distributions of response concerning the input can be illustrated using curves that depict the 16th, 50th, and 84th percentiles. (Fig. 14). The IDA curves and limit-state capacities across all records can be consolidated into 16, 50, and 84% fractiles based on the standard deviation (Fragiadakis and Vamvatsikos 2011) [8]. To enhance comprehension of the diverse effects of ground motion on numerical models, Figures 14(a) and 14(b) exhibits separate IDA curves and limit-state capacities across all records.

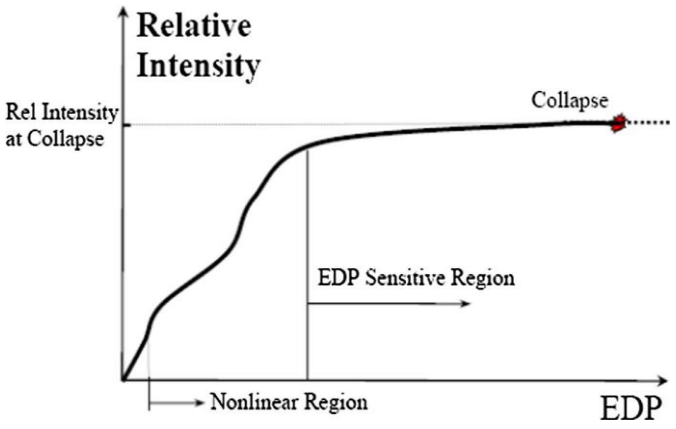

Fig. 1 EDP curve, relative intensity (Vamvatsikos and Cornell 2002)

1.2 Fragility Analysis

Upon the completion of the simulations and the determination of the maximum displacement at the top of the structure for each ground motion record, the initial step involved the computation of fragility functions. This necessitated the specification of limit states that characterize the performance of the structure. In order to assess the seismic damage states of the 8-story RC structure, the structural damage states were defined based on the allowable values of maximum inter-story drift ratios (IDRmax) of 1.0%, 2.0%, and 4.0%. These values correspond to the performance levels of Immediate Occupancy (IO), Life Safety (LS), and Collapse Prevention (CP), respectively. It is worth noting that the limit states were described according to Table C1-3 in (FEMA 356) [9]. Subsequently, the provided formula was utilized to calculate the fragility function (Baker JW 2015) [10], and the resulting plot is depicted in Figures 16(a) and 16(b). To enhance the practical applicability of the fragility functions, it is advisable to incorporate a more extensive set of ground motions, surpassing the 11 motions considered in this study. This approach ensures the development of reliable fragility functions, thereby facilitating accurate seismic performance and vulnerability assessments.

$$P\ (x \geq D) = 1-0.5\times(1+\mathrm{Erf}((\ln(D/\mu)/2\times\beta))$$

Where, P (x ≥ D) denotes the probability of exceedance of a specified damage state 'D' in terms of the defined EDP; Erf represents the Gaussian error function; 'β' is the standard deviation of the natural logarithm of the data points; 'μ' is the median of the EDP at the given ground motion, determined through exponential regression of user-entered data.

2. NUMERICAL MODELING

Ground story + 7 floor (G+7) Reinforced Concrete-Moment Resisting Frame is selected and designed according to (IS-456:2000) [11] and seismic load combinations are provided as per (IS-1893, Part 1: 2016) [12], and analyzed in ETABS 18.0.0. Dimensions of columns and beams are given in Table 1. The suite of 11 ground motion is selected for near-fault zone and far-field zone to study and compare the behavior of structure. The ground motion scaling is done by matching the response spectra for zone V with the ground motion accelerogram. The guidelines provided by (Najafi L. H. and Tehranizadeh, M.) [13], used for ground motion scaling for any type of soil and engineering demand parameters. The Incremental Dynamic Analysis is performed. For inelastic analysis the RC frame structure models are assigned with the proper plastic hinges in structural members like beams and columns. The beams are assigned to moment hinges only, and columns are assigned with the P-M-M hinges. The plastic hinges assigned to the elements are as per the (FEMA-356)

[9] and (ATC-40) [14] specified. The seismic response of the structure for higher modes is not considered as our structure as the effect of higher mode will be very less. The damping ratio is kept 5% as specified in (IS-18932002) [12]. There have been many reports on the influence of gravity effect on the calculated seismic response. In the present study, the effect of gravity loads is taken into account. Figure 2 depicts a structural schematic of a multi-story building, detailing the reinforcement of its concrete members. The term "b" represents the width of beams or columns, shown as 750 mm. "d" indicates their depth, varying between 120 mm and 90 mm. "s" refers to the spacing between longitudinal reinforcement bars within the members. "Ptot" is the total percentage of longitudinal reinforcement, and "Psh" denotes the percentage of shear reinforcement, both critical for the structure's stability and seismic resilience. Figure 2 and 3 shows elevation and plan view of the model structure. Figure 4 is a backbone curve for beam/column inelastic plastic hinge model according to (ASCE 41-13) [15]

Table -1: Describes Geometrical Configuration of G+7 Building Frame.

Dimensions of building	25 m x 35 m	
Height of structure	25.0 m	
Location	Guwahati, Assam State, India	
Bay spacing	5 m	
Number of bays	*X* direction	05
	Y direction	07
Storey height	First Storey	4.0 m
	Rest of the Storey's	3.0 m
Column Dimension	Column	750 mm x 750 mm
Beam Dimension	Beam	350 mm x 500 mm
Loading	Dead Load	Live Load
	5kN/m2	2.5kN/m2
Modulus of Elasticity	Concrete	Steel
	27386.13 MPa	200000 MPa
Thickness of slab	150 mm	
Earthquake Load	Zone factor: V Importance factor: 1 Response reduction factor: 5 Soil condition: Medium	
Grade of concrete	M30	
Grade of steel	Fe500 (Longitudinal bars)	Fe415 (Lateral ties)

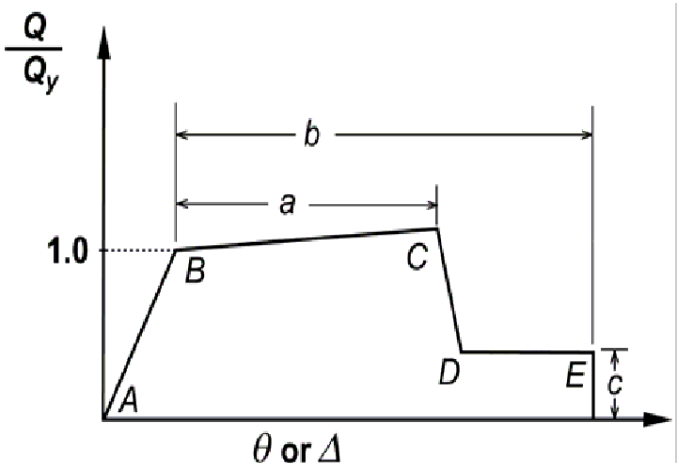

Fig - 4 Backbone curve for inelastic modeling

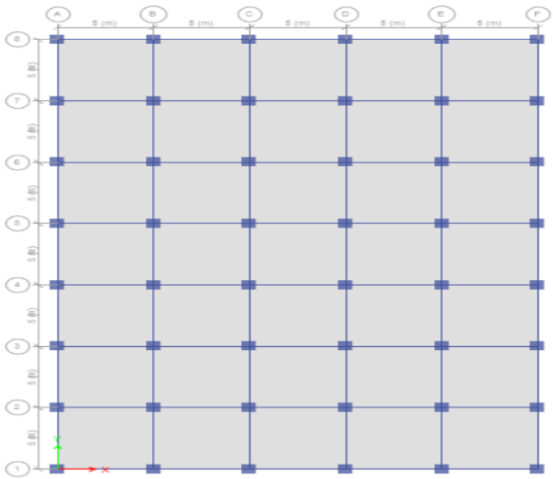

Fig - 3 Plan view of the building.

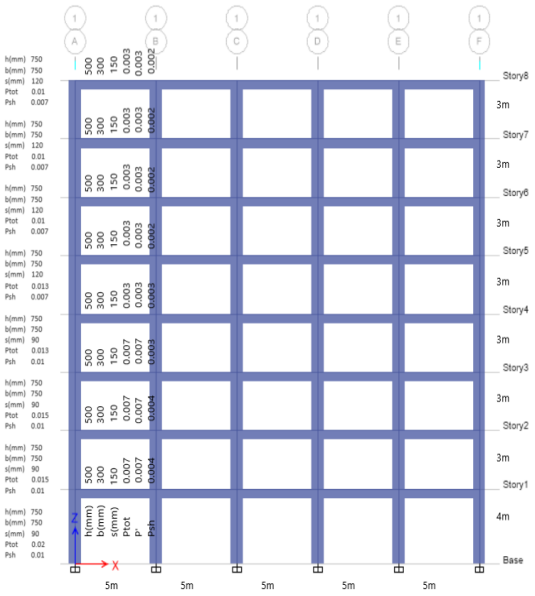

Fig – 2: Structural documentation of an 8-story building

3. GROUND MOTION SELECTION:

Eleven time-history loads of ground motion were utilized to account for the stochastic nature of the earthquakes. The data pertaining to the loading was provided to ETABS in the form of an acceleration file, which included the step size and the number of steps along the in-plane horizontal axis of the structure. The vertical component of the ground motion was disregarded. The data was procured from the PEER database [16]. The earthquakes were chosen in such a manner as to guarantee that the records accurately represent intense motion capable of causing structural collapse (Fabrizio, Paolacci 2023) [17]. Furthermore, certain minimum thresholds were imposed on the magnitude of the events, as well as the peak ground velocity and acceleration (C. Allin Cornell 2006) [18]. These thresholds were selected so as to strike a balance between the selection of significant motions and ensuring that a sufficient number of motions meet the selection criteria.

a) The magnitude of the earthquakes had to exceed 6.5.
b) The distance between the source and the site had to be greater than 10 km, which is the average of the Joyner-Boore and Campbell distances, for ground motions originating from far-field locations. For near-field ground motions, the distance had to be less than 10 km.
c) The peak ground acceleration had to exceed 0.2g and the peak ground velocity had to be greater than 15 cm/sec.
d) The shear wave velocity of the soil in the upper 30m, for NEHRP soil types A-D, had to be greater than 180 m/s. It should be noted that all the selected records happened to be on C/D sites.
e) There was a limit of six records from a single seismic event. If more than six records passed the initial criteria, then the six records with the largest peak ground velocity were selected. However, in some cases, a record with a lower peak ground velocity was used if the peak ground acceleration was significantly larger.
f) The lowest usable frequency had to be less than 0.25 Hz, in order to ensure that the low frequency content was not eliminated during the ground motion filtering process.
g) The faults considered were strike-slip and thrust faults.

The ground motions were chosen in accordance with the following rule: the average spectral acceleration response of all the considered ground motions should match or exceed and should not fall below 90% of the maximum considered earthquake with regards to risk over the period range of 0.2 to 2 times the highest natural period, T0, of the structure (Gandage, S., Salgado, R., and Guner, S. (2019) [19]. This rule is mandatory in modern codes for the structural analysis of seismic performance. Figure 5 displays the design spectral acceleration response of the wall, the maximum considered spectral response (MCR), the 0.2 to 2 times period range, and the 90% target line for the selection of ground motion. The selected ground motions are shown in Table 2 and 3.

Table 2 Documentation of selected far-fault ground motion records.

No.	Year	Earthquake	M_W	Station	PGA (g)
1	1976	Gazli, USSR	6.8	Karakyr	0.349
2	1979	Imperial Valley-06	6.5	Bonds Corner	0.438
3	1979	Imperial Valley-06	6.5	Chihuahua	0.501
4	1985	Nahanni, Canada	6.8	Site 1	0.363
5	1985	Nahanni, Canada	6.8	Site 2	0.415
6	1989	Loma Prieta	6.9	BRAN	0.364
7	1989	Loma Prieta	6.9	Corralitos	0.138
8	1992	Cape Mandocino	7.0	Cape Mandocino	0.233
9	1994	Northridge-01	6.7	LA—Sepulveda VA Hospital	0.464
10	1994	Northridge-01	6.7	Northridge-17645 Saticoy St	0.552
11	1999	Kocaeli, Turkey	7.5	Yarmica	0.871

Table 3 Documentation of selected near-fault ground motion records.

No.	Year	Earthquake	M_W	Station	PGA (g)
1	1994	Northridge	7.5	Baverly Hills - Mulhol	0.52
2	1999	Duzce, Turkey	7.4	Bolu	0.48
3	1979	Imperial-Valley	6.5	Delta	0.82
4	1987	Superstition Hills	7.0	El Centro	0.34
5	1999	Kobe, Japan	6.9	Nishi-Akashi	0.35
6	1992	Kocaeli, Turkey	7.37	Duzce	0.38
7	1989	Landers	7.4	Yermo Fire Station	0.51
8	1990	Loma Prieta	6.7	Capitola	0.24
9	1987	Manjil, Iran	6.7	Abbar	0.36
10	1999	LandersChi-Chi, Taiwan	7.3	CHY101	0.22
11	1976	Fruili, Italy	7.5	Tolmezo	0.24

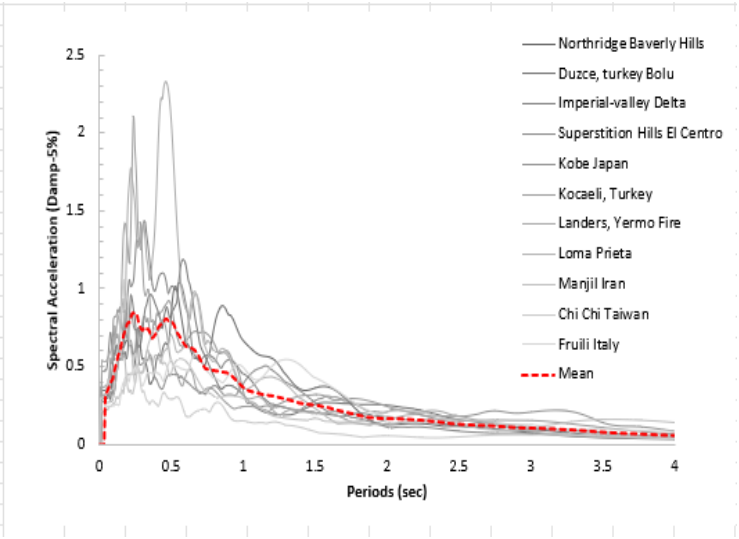

Fig. 6 Far-fault ground motions

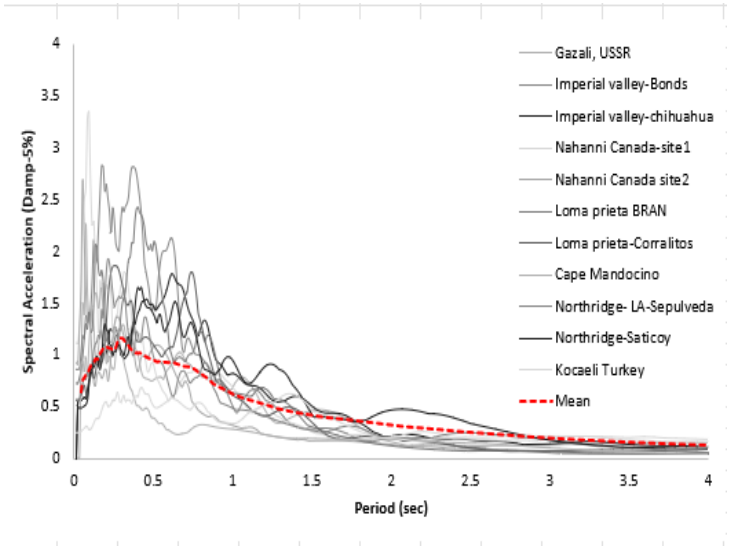

Fig. 7 Near-fault ground motions

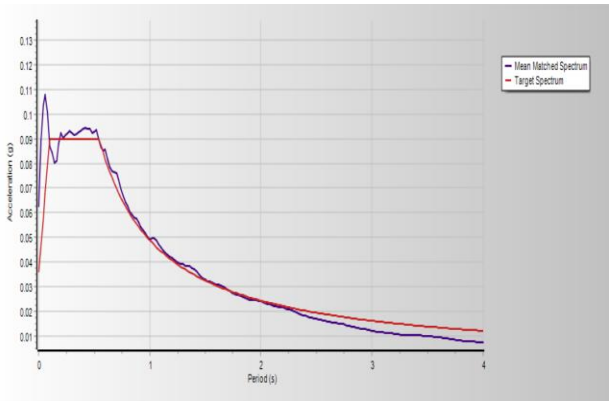

Fig. 8 Mean matched Far-field ground motions accelerograms with target spectrum.

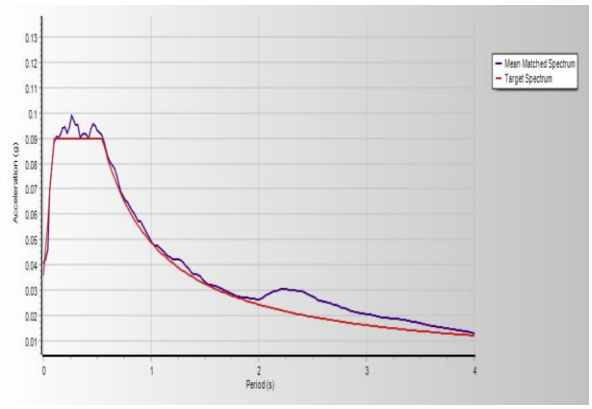

Fig. 9 Mean matched Near-field ground motions accelerograms with target spectrum.

5. RESULTS & DISCUSSIONS:

Here are the outcomes derived from the analyses performed on building models exposed to near-field and far-field ground motions. The study employs incremental dynamic analysis, encompassing the plotting and comparison of total story displacement, inter-story drift (IDR), and IDA curves. It's crucial to underscore that the building model undergoes scrutiny under both near-fault and far-fault ground motions, resulting in a total of 22 nonlinear time history analyses. The seismic demand parameter used is the inter-story drift ratio, which signifies the displacement between adjacent floors divided by the story height. The nonlinear time history analysis reveals the results for an 8-story building model with a moment frame, showcasing the maximum lateral displacement under both near-fault and far-fault ground motions. It's noteworthy that far-fault motions generally entail consistent lateral displacement requirements. In contrast, near-fault conditions necessitate higher requirements.

5.1 Seismic Response Evaluation of Buildings

The relative displacement between stories plays a pivotal role in determining the structure's failure rate, making it a crucial metric for seismic performance assessment. Upon comparing the average maximum inter-story drift ratios (IDR) under both far and near-field ground motions, a significant difference is evident. Specifically, the maximum inter-story drift is observed to be 30 mm, marking a 33 percent increase compared to the 22.5 mm recorded under far-field conditions. Additionally, the maximum story displacement is 235 mm, indicating a 46 percent increase in comparison to the 160 mm observed in the far-field scenario. The drift pattern during a far-field earthquake exhibits a more uniform distribution with less variation among different stories, signifying a consistent behavior throughout the building's height. In contrast, the near-field earthquake manifests a greater fluctuation in drift between stories, particularly at the upper levels. This observation suggests a

more pronounced influence of the near-field seismic characteristics on the building's response.

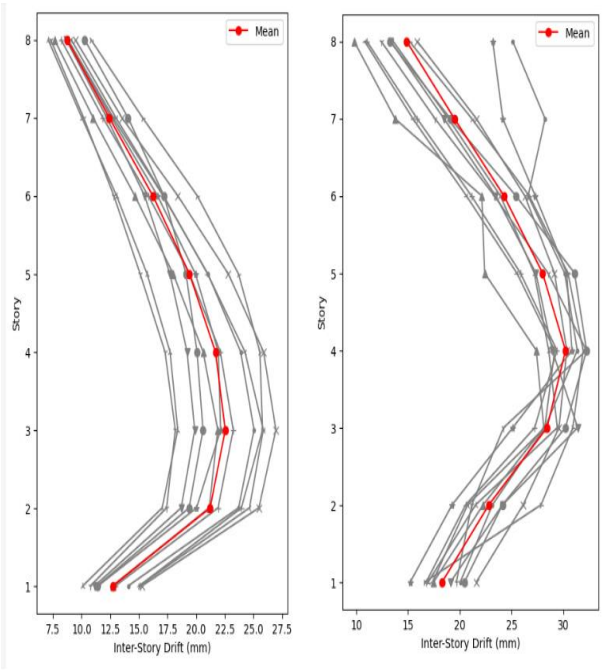

Fig. 10 and 11 Seismic Responses for 8-storey RC frame; under far-fault and near fault ground motions

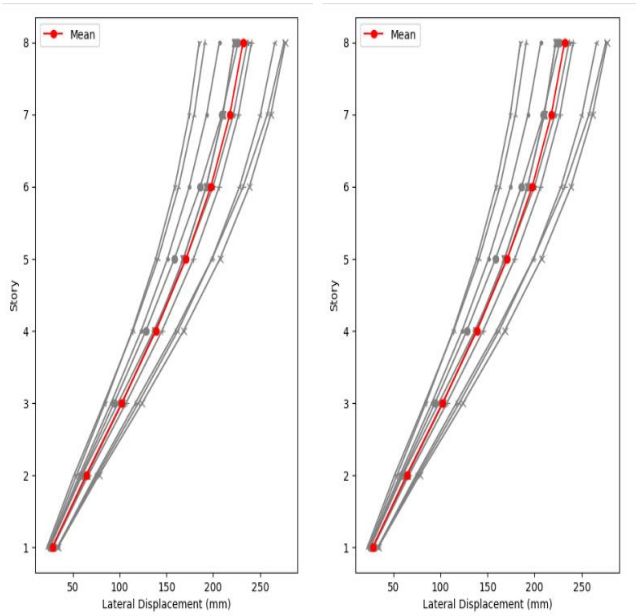

Fig. 12 and 13 Seismic responses for 8-storey RC frame under far and near fault ground motions

5.2 Incremental Dynamic Analysis Results (IDA curves)

The results of Incremental Dynamic Analysis for far-fault and near-fault earthquake scenarios is shown figure 14(a) exhibits higher spectral accelerations at corresponding inter-story drift levels compared to figure 14(b) indicating that the structure has a more responsive or stiffer seismic response. The pronounced divergence between the 16% and 84% lines in fig 14(a) denotes a greater variability in the seismic response, which could be attributed to factors such as varying dynamic properties of the building, different modes of vibration being excited, or a broader range of possible earthquake inputs within the far-field spectrum. Conversely, fig 14(b) presents a more condensed confidence interval between the 16% and 84% lines, which translates to a more predictable and consistent structural behavior under near-field seismic conditions. This could imply that the building has a more uniform performance or that the near-field earthquake records possess less variability in terms of frequency content that resonates with the building's natural frequencies. Furthermore, the peak spectral acceleration values in fig 14(a) surpass those in fig 14(b), which suggests that the building might experience higher forces during seismic events. This could be consequential for the design and detailing of structural components, as it implies a need for greater strength and ductility to withstand these forces. In essence, the IDA curves demonstrate that the structure subjected to far-field earthquake scenarios requires consideration for a higher range of seismic forces and a more variable response, potentially necessitating a more robust design approach. On the other hand, the structure subjected to near-field earthquake scenarios, shows a more uniform and less forceful response, possibly allowing for a design that can be more finely tuned to a narrower range of expected seismic actions.

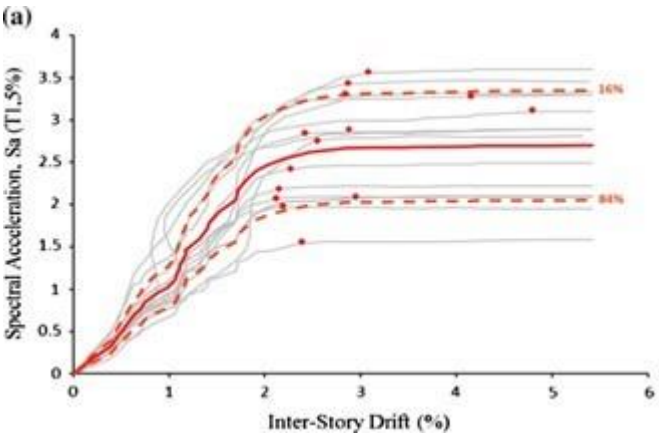

Fig. 14(b) IDA curves for 8-storey structure: (a) far-field earthquake records

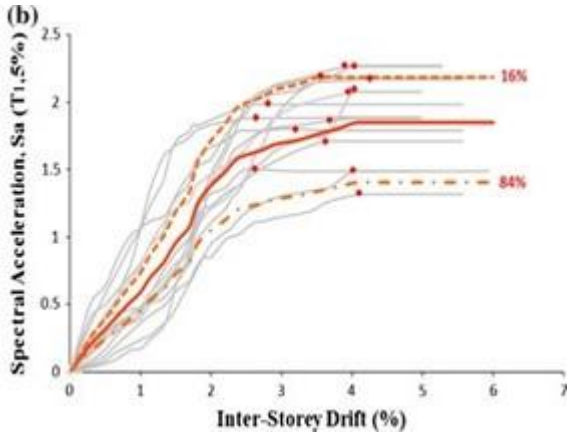

Fig. 14(b) IDA curves for 8-storey structure: (b) near-field earthquake records

5.3 Fragility Curves

In seismic analysis, the distinction between near-fault and far-fault seismic effects plays a crucial role in understanding structural behavior. Far-fault seismic motions, illustrated in Figure 1, are characterized by lower-frequency content and the absence of a distinct pulse. The energy input into structures occurs gradually and is spread out over a more extended duration. The fragility curves in Figure 1 demonstrate a more gradual increase in the probability of exceedance with rising spectral acceleration. This is attributed to the far-fault motions having a less immediate impact on structures, allowing for increased energy dissipation over time. Understanding these distinctions is essential for designing structures resilient to various seismic scenarios. On the other hand, Near-fault seismic effects Far-fault seismic motions, as depicted in Figure 2, exhibit high-frequency content and a pulse-like velocity waveform. These characteristics can exert significant demands on structures, particularly those with a resonant natural period. The fragility curves in Figure 2 (IO to CP) illustrate this behavior, emphasizing the steep initial slopes. Even a slight increase in ground motion intensity can substantially raise the probability of exceeding a limit state, aligning with the rapid and intense ground motions associated with near-fault earthquakes.

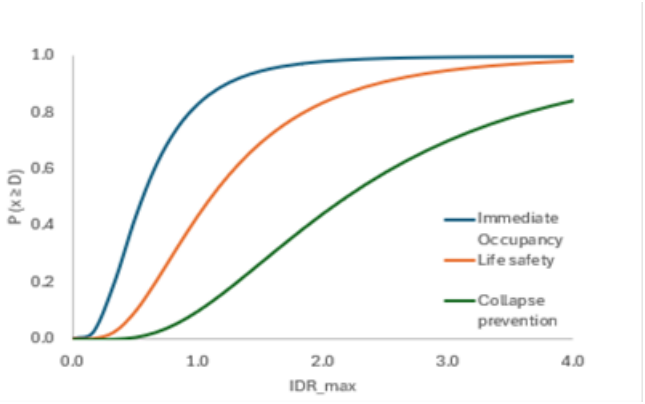

Fig. 16(a) Fragility curves for 8-storey structure; (a) far-field earthquake records

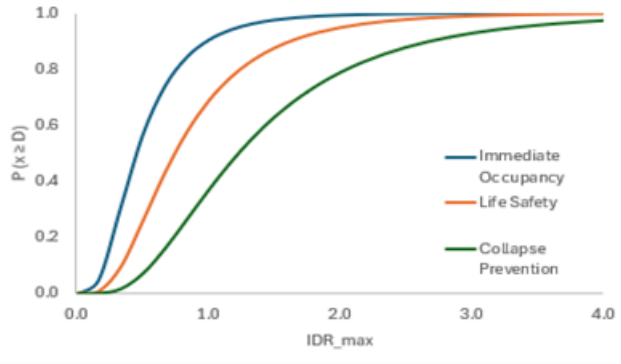

Fig. 16(b) Fragility curves for 8-storey structure; (b) near-field earthquake records

6. CONCLUSION:

This research undertook an examination of the seismic performance of reinforced concrete buildings exposed to near- and far-fault ground motions using incremental dynamic analysis techniques. The scrutiny concentrated on an 8-story building situated on stiff soil. Numerical simulations revealed that the influence of velocity pulses in the velocity time history led to substantial deformations in reinforced concrete buildings, necessitating considerable energy dissipation within one or more cycles of Structural Plastics Limited. This requirement-imposed limitations on the structure's ductile capacity. Conversely, far-fault motions gradually introduced input energy. Although, on average, deformation demands were lower than those in near-fault scenarios, structural systems underwent more plastic cycles. As a result, the cumulative effects of far-fault records were minimal.

Modeling outcomes indicated that, for two earthquakes with nearly identical conditions, greater displacement values were observed in near-fault scenarios. Notably, near-fault ground motions exhibited higher recorded drift than far-field ground motions for the same level of intensity measure, a

phenomenon attributed to differences in spectral acceleration. Near-fault ground motions demonstrated higher spectral acceleration compared to those in the far field. Consequently, the structure experienced increased drift with a relatively smaller increment of Intensity Measure (IM) in the case of near-fault ground motions.

The implications of this study for seismic design and retrofitting suggest that different strategies may be necessary depending on the proximity to the fault. Near-fault seismic design might require specific considerations for energy dissipation and control mechanisms to address the initial shock and velocity pulse, while far-fault design may prioritize overall energy input and ductility to handle longer-duration shaking.

REFERENCES

[1] (Erdik, M., B. Şadan 2023). Near-Fault Earthquake Ground Motion and Seismic Isolation Design. doi: 10.1007/978-3-031-21187-4_9

[2] Bhairav, Thakur., Atul, K., Desai., Hemal, J, Shah., Gondaliya, Kaushik. (2022). Innovative Probabilistic Vulnerability Investigation of Nuclear Power Plant Structures under Far-Field Ground Motion. Disaster Advances, doi: 10.25303/1601da14022

[3] V., Bui, Tran., Son, T, Mr., Nguyen., Van, Hap, Nguyen., T.-H., Doan., Duy-Duan, Nguyen. (2022). The Influence of Near- and Far-field Earthquakes on the Seismic Performance of Base-Isolated Nuclear Power Plant Structures. doi: 10.48084/etasr.5156

[4] Renato, Giannini., Fabrizio, Paolacci., Hoang, Nam, Phan., Daniele, Corritore., G, G, Quinci. (2022). A novel framework for seismic risk assessment of structures. Earthquake Engineering & Structural Dynamics, doi: 10.1002/eqe.3729

[5] (2022). Characterization of site location versus the causative fault in seismic demands of structures. Structures, doi: 10.1016/j.istruc.2022.04.062

[6] Vmvatsikos D, Cornell CA (2002) Incremental dynamic analysis. Earthq Eng Struct Dyn 31(3):491–514

[7] Vamvatsikos D, Cornell CA (2004) Applied incremental dynamic analysis. Earthq Spectra 20(2):523–553

[8] Fragiadakis M, Vamvatsikos D (2011) Qualitative comparison of static pushover versus incremental dynamic analysis capacity curves. In: Proceedings of the 7th hellenic national conference on steel structures, Volos

[9] FEDERAL EMERGENCY MANAGEMENT AGENCY-356: Pre-standard and Commentary for Seismic Rehabilitation of Buildings. Washington, 2000, pp. 1-35.

[10] Baker JW (2015) Efficient analytical fragility function fitting using dynamic structural analysis. Earthq Spectra 31(1):579–599

[11] IS 456: Plain and Reinforced Concrete—Indian Standard Code of Practice. Bureau of Indian Standards, New Delhi, 2000, pp. 1-114.

[12] IS 1893 (Part 1). Earthquake loading, Bureau of Indian Standards, New Delhi, 2016, pp. 1-44.

[13] NAJAFI, L. H. – TEHRANIZADEH, M.: Ground Motion Selection and Scaling in Practice. Periodica Polytechnica Civil Engineering, Vol. 59, 2015, pp. 233-248.

[14] Applied Technology Council, ATC-40 (1996) Seismic Evaluation and Retrofit of Concrete Buildings, Vols. 1 and 2, California.

[15] ASCE 41-13.: Seismic Evaluation and Retrofit of Existing buildings. American Society of Civil Engineers, Virginia, 2013, pp. 1-12.

[16] https://peer.berkeley.edu/peer-strong-ground-motion-databases

[17] Fabrizio, Paolacci., Renato, Giannini., Phan, Hoang, Nam., Daniele, Corritore., G, G, Quinci. (2023). Scores: an algorithm for records selection to employ in seismic risk and resilience analysis. Procedia structural integrity, doi: 10.1016/j.prostr.2023.01.040

[18] Jack, W., Baker., C., Allin, Cornell. (2006). Spectral shape, epsilon and record selection. Earthquake Engineering & Structural Dynamics, 35(9):1077-1095. doi: 10.1002/EQE.571

[19] Gandage, S., Salgado, R., and Guner, S. (2019) "FFG: Fragility Function Generator," Macro-Enabled Excel Spreadsheet, Department of Civil and Environmental Engineering, The University of Toledo, Ohio, USA